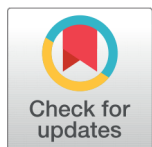


RESEARCH ARTICLE

 OPEN ACCESS

Received: 30-01-2024

Accepted: 29-02-2024

Published: 14-03-2024

Citation: Deokar R, Banpurkar AG, Singh AR, Mehta J, Gajengi A, Thatai S, Pahwa N, Nalawade S (2024) Morphological, Optical and Voronoi Polygon Analysis of Breath Figures Prepared on Polymeric Surface. Indian Journal of Science and Technology 17(12): 1180-1188. <https://doi.org/10.17485/IJST/v17i12.259>

* **Corresponding author.**arvind.singh@gnkhalsa.edu.in**Funding:** None**Competing Interests:** None

Copyright: © 2024 Deokar et al. This is an open access article distributed under the terms of the [Creative Commons Attribution License](https://creativecommons.org/licenses/by/4.0/), which permits unrestricted use, distribution, and reproduction in any medium, provided the original author and source are credited.

Published By Indian Society for Education and Environment ([iSee](https://www.isee.org/))

ISSN

Print: 0974-6846

Electronic: 0974-5645

Morphological, Optical and Voronoi Polygon Analysis of Breath Figures Prepared on Polymeric Surface

Rajashree Deokar^{1,2}, Arun G Banpurkar², Arvind R Singh^{1*}, Jignesh Mehta¹, Aravind Gajengi³, Sheenam Thatai⁴, Neelam Pahwa⁵, Sandipan Nalawade¹

1 Department of Physics, G. N. Khalsa College, Matunga, Mumbai, 400019, Maharashtra, India

2 Department of Physics, Savitribai Phule Pune University,, Pune, 411007, Maharashtra, India

3 Department of Chemistry, Ramnarain Ruia Autonomous College, Matunga, Mumbai, 400019, Maharashtra, India

4 Department of Chemistry, Amity Institute of Applied Sciences, Amity University, Noida, 201313, Uttar Pradesh, India

5 Department of Electronics, Zakir Husain Delhi College, University of Delhi, J.L.N. Marg, 110001, New Delhi, India

Abstract

Background/Objectives: The formation of breath figures over polymers like polystyrene has vast applications in material science for making numerous micro- and nanopatterned functional surfaces. However, the breath figures (BFs) method is a complex phenomenon as the actual formation of structures are many times unpredictable and the nature of structure depends on the type of polymer, solvent, degree of humidity and additives used. The work presented in this paper deals with the study of condensation on the surface of volatile polystyrene polymer solution and their uses for non-wetting using optical and morphological studies along with mathematical model Voronoi polygon analysis using polystyrene and solvent of benzene and chloroform. The growth dynamics of Breath-Figures (BFs) formed due to condensation is presented in brief. **Method:** Breath Figure (BF) patterns were prepared by two solvents: benzene and chloroform. Different representative values of relative Humidity viz. 60, 70, 80 and 90 % were employed for making BFs. Two different polymer concentrations of 5 and 10 w/v % was used in this study. **Findings:** The morphology has been statistically analyzed for different parameters like average diameter and their size distribution etc. In case of BFs formed on benzene surface, droplet has average diameter of about 12 μm at 90% humidity but in case of chloroform surface this diameter is about 25 μm at 90% humidity. Voronoi analysis demonstrates simplistic way to qualitatively check the six-fold order and the coordination numbers in BFs. **Novelty:** The work shows comparative study of BFs patterns using polystyrene on two different solvents with changing humidity. The study shows morphology of the breath patterns is mainly dependent on the polymer concentration, humidity and density of solvents which is a new observation. The study leads to the acquisition of new

knowledge on BFs which provides insight important for various applications including biological fields.

Keywords: Breathfigures; Voronoi polygon; Polystyrene; Contact angle; Condensation

1 Introduction

Fabrication of droplet structures similar to porous structures on polymer via breath figure approach have tremendous application such as catalysis, immobilization of active substances in food, functional protein, and enzyme immobilization⁽¹⁾. Hence, fabricating them in a simple and controlled manner, with size scalability is of interest. A simple, cost-effective, single-stage method for the fabrication of porous polymer films is breath figure (BF) approach⁽²⁾. The wetting property of solid would be playing a crucial role in the process of condensation. The wetting property can be changed by surface roughness, introducing chemical heterogeneity and surface impurities or contamination. Condensation of water molecules on a cold surface forming tiny droplets is a common process in nature and it is called Breath figure. The “Breath figure” name comes from formation of beautiful breath pattern on clean glass in winter season. Also, another example of breath figure is surface fog. Breath figures are formed due to condensation of water vapor on cold surfaces. Normally, the morphology of condensate disappears after evaporation of water. To retain these impressions, a small amount of polymer is often added in volatile solvent to preserve breath figures impression after water evaporation⁽³⁾. After evaporation of the volatile solvent, the impression of water droplet i.e.i.e., breath figure remains fixed on polymer surface for longer duration. The physical properties of volatile solvents such as vapor pressure, latent heat of evaporation, surface tension and solvent density are more crucial⁽⁴⁾. Several kinds of solvents are used such as carbon disulfide, benzene, toluene, chloroform, ethyl acetate, 1-2 dichloromethane and dichloromethane also polymers like polystyrene are added in the solvents to obtain films with wide range of porosity features.

BFs formation has been explored by many researchers using different polymers and employing variation of physical parameters to obtain different structures in terms of size from micro to nano. The images of BFs shows quantitative variation which has to be studied quantitatively using several mathematical models. Quantitative parameters of self-organization can be obtained by building the Voronoi diagram (also called the Voronoi tessellation, or Voronoi partition) and calculating the appropriate Voronoi entropy⁽⁵⁾. In this work a detailed quantitative analysis of Voronoi polygon analysis has been done for BFs produced. BFs of different having tuned dimension are utmost important and work has been carried out by several researchers on different polymers to obtain different tunable sizes of structures⁽⁶⁾. Researchers have explored the effects of variation of solvent for formation of BFs and have found direct evidence of it on formation of BFs with different size.^(7,8) It has also been seen that humidity and concentration plays a very important role in the formation of BFs.⁽⁹⁾ Contact angle and SEM images plays a very important role in studying the BFs and they provide help and data for several mathematical analysis studies^(5,6). The work presented in this paper deals with the study of condensation on the surface of volatile polymer solution and their uses for non-wetting surface using Voronoi polygon analysis and morphological studies.

2 Methodology

2.1 Experimental Techniques

Prior to casting a polymer drop on glass surface for BF formation, microscopic glass substrates were cleaned by adopting standard cleaning procedure. The piece of microscopic glass slides typically ($1 \times 3 \text{ cm}^2$) were ultrasonically cleaned using trichloroethylene (C_2HCl_3 , Thomas Baker) for five minutes to remove any organic impurities. Further they were cleaned in ultrasonic bath with acetone for same duration and rinsed in iso-propyl alcohol bath. These substrates were dried gently in nitrogen gas flow and kept in oven at 60°C for 30 minutes.

2.1.1 Preparation of polymer solution with different concentrations

Commercially available polystyrene beads (Sigma-Aldrich, with M.W. 192 K) were dissolved separately in chloroform and benzene solvents (analytical grade, Thomas Becker, India). The solutions of different weight concentration ranging from 5 w/v % and 10 w/v % were prepared, and they were kept stirring for 3-4 hour to ensure homogeneous polymer solution. These clear solutions were used for drop casting and breath-figure formation.

2.1.2 Drying of colloidal suspension on breath figure surface

Colloidal microsphere solution was used to perform experiments. The polystyrene beads (Polyscience, Inc) of two different diameters (0.5 and 2 μm) were used to perform experiment. In brief, a diluted solution was prepared from one drop of microsphere dispersed in a freshly prepared 5 mL of distilled water and stirred it well. For both the time, similar procedure was followed to get desired solutions. A 2-3 μL drop of this solution was casted on BF substrates and allowed it to dry at room temperature. These samples were extensively characterized further using optical microscopy technique.

2.2 Characterization Technique

2.2.1 Optical Morphology Measurement

In this study optical microscopy is mainly utilized for characterizing morphology. The images of the BF patterns were captured using CMOS camera (UI1250 ML-C-HQ, IDS, Germany) attached to an optical microscope (Leitz-Wetzlar, Germany) in upright transmission mode. Breath figure patterns were captured mainly from the central region of polystyrene film, which was left behind after the evaporation of the volatile fluid in the droplet region⁽⁵⁾.

2.2.2 Contact Angle Measurement

Contact angle measurement has been found to be an indispensable technique for surface characterization and wettability study due to its simplicity⁽⁶⁾. The instrument used in this work was optical contact angle goniometer with image processing software (SCA20, data physics, Germany). The experiments were carried out at room temperature, $20\text{--}22^\circ\text{C}$ and at relative humidity of 50 %. Experimentally, when a liquid is contacted with solid and other phases, it is usually observed that the contact angle does not reach its equilibrium value instantaneously. Here, we measure contact angle by casting a water drop of known volume with the help of micropipette.

3 Results and Discussion

3.1 Morphology of breath figure

The polymer solution in benzene and Chloroform was drop-casted in a humidified chamber and allowed to form a breath figure on the surface of polymer solution. After complete evaporation of the volatile solvents, the impression of condensate droplet (breath figure) is remained on polymer surface in the form of hemispherical dimples. Such surfaces were analyzed for surface morphology. Figures 1 and 2 show breath figure (BF) patterns for the cases of benzene and chloroform solvents and for different representative values of relative Humidity viz. 60, 70, 80 and 90 %. Two different polymer concentration 5 and 10 w/v % was used in this study. After a complete drying of liquid, BF patterns were captured using optical microscope at 10x magnification using CCD camera and these digitalized images were analyzed using open-source ImageJ software. As seen from Figures 1 and 2 one can visually notice that the ordering of the droplets is quite uniform like two dimensional closed packed structures with few defects. However, in the case of chloroform, the ordering of the droplets is less pronounced in comparison to the case of benzene. Figure 3 shows variation of pore diameter verses humidity. Morphological data are in tune with available literature with providing more detailed analysis and the present data shows better morphological variation with humidity for two different solvents. Close observation reveals that there is a difference in BF patterns mainly in droplet size distributions as

well as in the droplet morphology^(6,9). It is seen that concentration of the polymer in solution is significantly affecting droplet morphology. A higher concentration of polymer shows an increase in droplet density and uniformly distributed droplets (see Figure 2). Figure 3 (a-b) shows plot of average droplet diameter versus humidity value for benzene and chloroform solution respectively. It is seen that in both cases, droplet diameter linearly increases with humidity. In case of BF formed on benzene surface, droplet has average diameter of about $12\ \mu\text{m}$ at 90% humidity but in case of chloroform surface this diameter is about $25\ \mu\text{m}$ at 90% humidity. This effect is also seen in average density of droplets. In the case of benzene, density of droplets is higher compared to density in case of BF formed using chloroform solvent. The packing of droplets of large radius leads to more voids and hence number of droplets accommodating in the unit area decreases. It is observed that secondary growth of BF is not significant in both cases. Only the size of primary droplets is increasing by the coalescence of neighboring droplets^(10,11). The above results are in good agreement with available literature which shows there is direct effect of solvent on morphology of prepared BFs.⁽¹²⁾

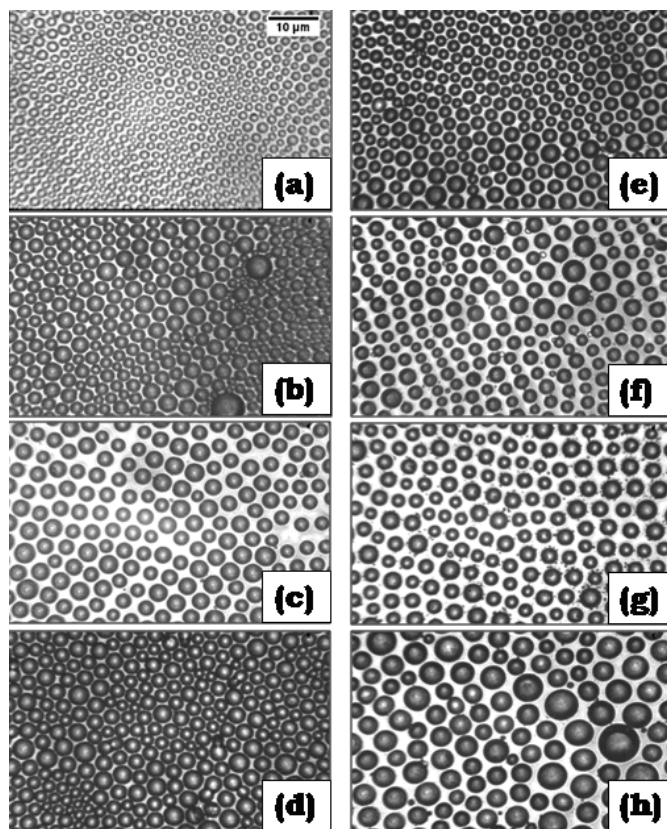


Fig 1. Breath figures (polymer conc. = 5 w/v %) patterns on the surface of benzene (a)-(d) and chloroform (e)-(h) droplets with respective humidity values

3.2 Voronoi polygon analysis

A Voronoi tessellation or diagram of an infinite plane is a partitioning of the plane into regions based on the distance to a specified discrete set of points (called seeds, sites, nuclei, or generators). For each seed, there is a corresponding region consisting of all points closer to that seed than to any other. The Voronoi polyhedron of a point nucleus in space is the smallest polyhedron formed by the perpendicularly bisecting planes between a given nucleus and all the other nuclei. The Voronoi tessellation divides a region into space-filling, non-overlapping convex polyhedral^(5,13). The droplet morphology was further analyzed for number of the nearest neighbor droplet and periodicity in the BF droplet using Voronoi polygon. As a representative case, a detailed analysis was carried out for 80 % relative humidity for both benzene and chloroform solution. Voronoi polygon analysis demonstrates simplistic way to qualitatively check the six-fold order and the coordination numbers in BFs. The coordination number (z) is defined as the number of its nearest neighbors. In case of a perfect hexagonal lattice, all the pores are the number

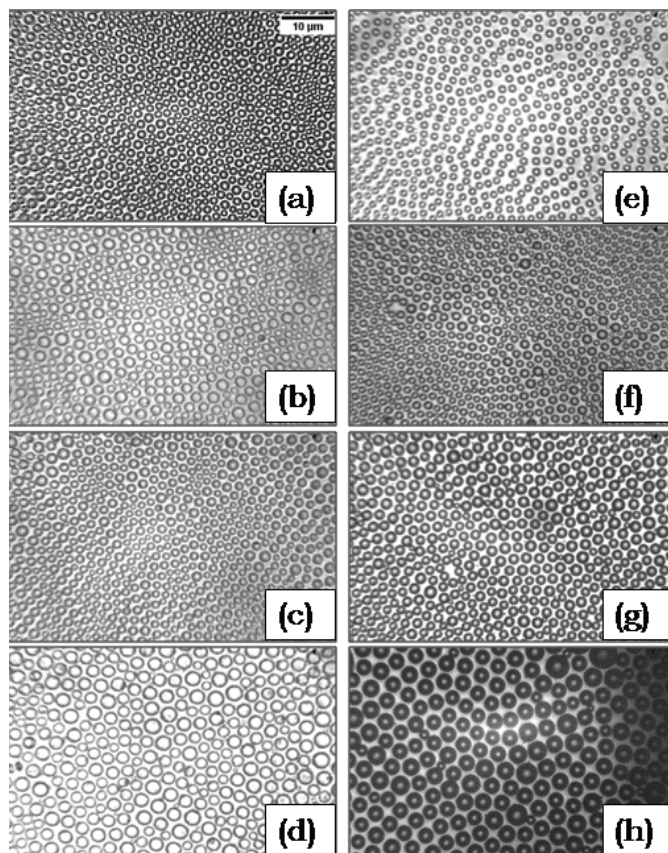


Fig 2. Breath figures (polymer concentration= 10 w/v %) patterns on the surface of benzene (a)-(d) and chloroform (e)-(h) droplets with respective humidity values

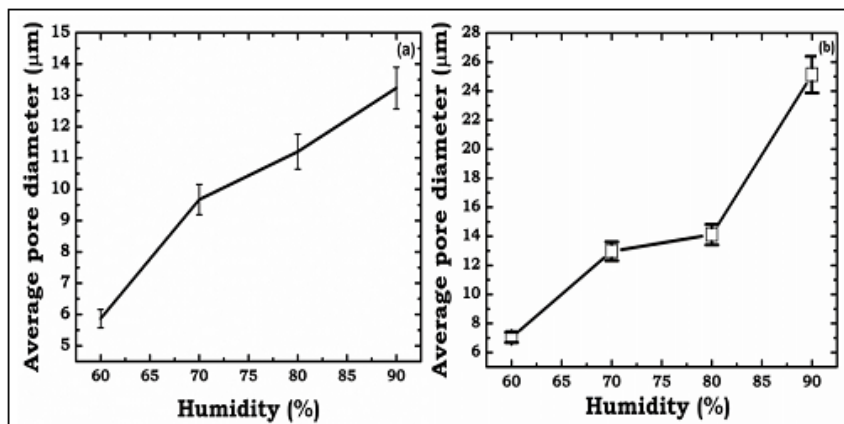


Fig 3. Average pore diameter vs Humidity (a) benzene (b) chloroform for 5% polymer concentration

of its nearest neighbors and P_6 should be one⁽²⁾. To determine which pores are neighbors, we used a method based on Voronoi polygons, Voronoi cell (or Dirchlet region) is the convex polygon surrounded by a point, whose sides are perpendicular bisectors of lines between the points and its nearest neighbors which is shown in Figures 4 and 5⁽¹⁴⁾.

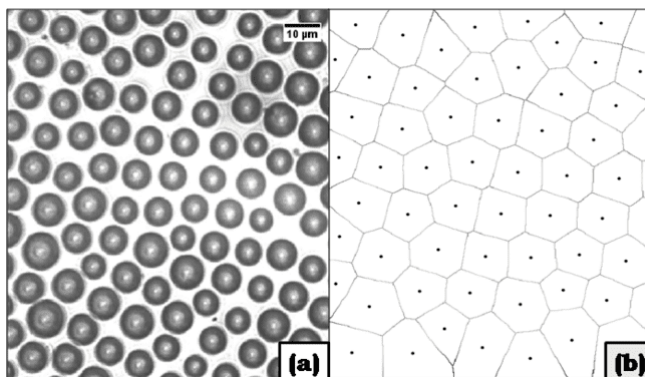


Fig 4. Breath figure pattern on (a) benzene surface and (b) voronoi polygon construction for the same pattern

An analysis of Voronoi construction was made in terms of the coordination number (n) of a polygon, which is the number of sides of a Voronoi polygon and P_n is the fraction of number of polygons having the coordination number n . The salient features of Voronoi polygon are (a) The segments of the Voronoi polygon are all the points in the plane that are equidistant to the nearest sites and (b) The Voronoi nodes are the points that are equidistant to three or more sites⁽¹⁵⁾.

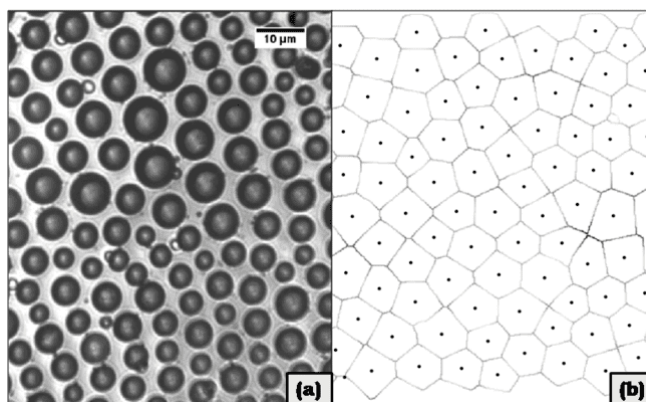


Fig 5. Breath figure pattern on (a) chloroform surface and (b) Voronoi polygon construction for the same pattern

The percentage values of P_4 , P_5 , P_6 and P_7 in case of benzene were found to be 0.166, 0.250, 0.583 and 0.147. The same in case of chloroform were respectively found to be 0.163, 0.295, 0.459 and 0.104. For comparison, a distribution for the case of a random configuration of points has been plotted in Figure 6. Similar observations in variation of percentage values due to change in physical parameters have also been reported in literature^(16,17), however the data shown in this study is in more detailed information.

As discussed above, by changing polymer concentration and humidity, there is change in diameter of pores as well. This results in micrometer rough surface which can be utilized for (a) water repellent surface and (b) micrometer sized petri-plates for cell culture. In the following section we present detailed analysis on wetting property on BF surface using optical contact angle (OCA) goniometer^(17,18).

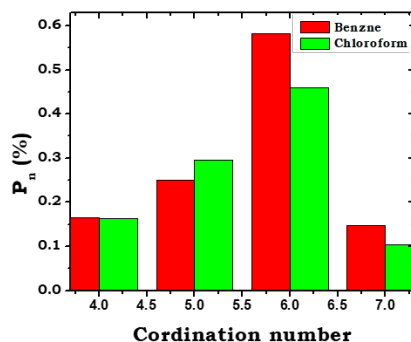


Fig 6. The fraction of P_n of Voronoi polygons of coordination (n) vs n is plotted for Benzene and Chloroform solvent

3.3 Contact angle measurements

Contact angle measurement technique provides information related to the ability of liquid to spread on the given surface. Usually for the plane surface it is defined by Young's equation:

$$\cos \theta_Y = \frac{\gamma_{SV} - \gamma_{SL}}{\gamma_{LV}} \quad (1)$$

where γ_{ij} being surface energy of the i^{th} liquid (solid) in presence of j^{th} solid (liquid). For the rough surface the apparent contact angle θ^* can be defined by Wenzel model as:

$$\cos \theta^* = r \cos \theta_Y \quad (2)$$

where r is roughness factor defined as the ratio of actual surface area to the projected area. This is always greater than 1 for rough surface and 1 for a flat surface.

In the present case the flat polystyrene are surfaces prepared from benzene and chloroform without humidity shows water contact angle (WCA) higher than 90° (19). Hence, any roughness on a polystyrene (PS) surface will enhance apparent WCA. The CA measurements were carried out using 5 ml drop of distilled water. A water drop was gently placed on the breath figured polystyrene substrates prepared from benzene and chloroform solution and contact angle was measured using Optical contact angle (OCA). From Figure 7 of WCA for different humidity level, it is seen that the highest CA was observed for BF surface prepared at 90% humidity. For comparison, we have plotted a graph of apparent Contact angle (CA) with respect to humidity for PS surface prepared from benzene and chloroform solvents.

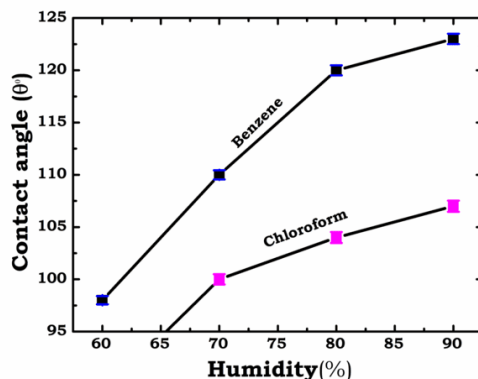


Fig 7. Water Contact Angle (WCA) on breath figured surface prepared at different Humidity level

Experimental data clearly demonstrate that pore size of breath figures can be controlled by both solvents and film processing conditions, mainly humidity. The variation in CA is also shown as a function of pore size which can be controlled by the

humidity condition. The increase in contact angle is due to interaction of droplet molecules due to variation in humidity which has also been reported in literature^(20–22). Several researchers have obtained the variation in contact angle by varying different physical parameters such as temperature and other^(23,24). In this study we obtained desired variation by changing the humidity which is very easy and simple.

In the following Table 1, we summarize results on breath figures on polystyrene surface prepared from solution in benzene and chloroform in the controlled humidity condition.

Table 1. Quantitative features of BFs pattern on the surface of benzene and chloroform

Sr no	Humidity (%)	Average Pore diameter (mm)		Surface coverage (%)	
		Benzene	Chloro-form	Benzene	Chloro-form
1	60	5.9	7.1	0.792	0.729
2	70	9.8	13.2	0.725	0.806
3	80	11.3	15.50	0.721	0.775
4	90	13.4	23.1	0.742	0.705

4 Conclusion

The above work shows comparative study of BF patterns on two different solvents with changing humidity revealing the insight for obtaining tunable BFs structures with required pore size and its detailed analysis was successfully carried out. The morphology data predicts that the formation of breath patterns is mainly dependent on the polymer concentration, humidity, and density of solvents. During the breath figure formation i.e. condensation of water vapor on benzene, the droplet sinks in the solution due to low density of solvent. This process reduces the rate of droplet coalescence, hence more ordered arrangement of droplet is seen in the case of benzene. However, such order of droplets is less in the case of chloroform solution. Voronoi construction for analyzing the nature of patterns is employed. In both the cases, the probability of six nearest neighbors is highest.

References

- Zhang S, Peng B, Li M, Diao H, Wang X, Zhao W, et al. Immobilization of Active Substances in Food Using Self-Organized Patterned Porous Film via Breath Figure Approach. *ChemistrySelect*. 2021;6(5):1067–1072. Available from: <https://doi.org/10.1002/slct.202004827>.
- Swathi PV, Madhurima V. Porous polymer film formation by water droplet templating using polystyrene. *The European Physical Journal E*. 2023;46(4). Available from: <https://doi.org/10.1140/epje/s10189-023-00282-x>.
- Dent FJ, Harbottle D, Warren NJ, Khodaparast S. Temporally Arrested Breath Figure. *ACS Applied Materials & Interfaces*. 2022;14(23):27435–27443. Available from: <https://doi.org/10.1021/acsami.2c05635>.
- Ananthakeshava I, Srikanth NJ, Prasad KN, Vinu V. Reduction in Surface Tension of Water Due to Pranik Healing. *Indian Journal of Science and Technology*. 2021;14(26):2175–2179. Available from: <https://doi.org/10.17485/IJST/v14i26.488>.
- Frenkel M, Fedorets AA, Dombrovsky LA, Nosonovsky M, Legchenkova I, Bormashenko E. Continuous Symmetry Measure vs Voronoi Entropy of Droplet Clusters. *The Journal of Physical Chemistry C*. 2021;125(4):2431–2436. Available from: <https://doi.org/10.1021/acs.jpcc.0c10384>.
- Rajaram M, Kandasamy S, Ravichandran A, Muthadhi A. Effect of Polystyrene Waste on Concrete at Elevated Temperature. *Indian Journal of Science and Technology*. 2022;15(38):1912–1922. Available from: <https://doi.org/10.17485/IJST/v15i38.225>.
- Zhang X, Wang B, Huang L, Huang W, Wang Z, Zhu W, et al. Breath figure–derived porous semiconducting films for organic electronics. *Science Advances*. 2020;6(13):1–9. Available from: <https://doi.org/10.1126/sciadv.aaz1042>.
- Estimé ML, Schindler M, Shahidzadeh N, and DB. Droplet Size Distribution in Emulsions. *Langmuir*. 2024;40(1):275–281. Available from: <https://doi.org/10.1021/acs.langmuir.3c02463>.
- Wong WHB, Janssen PJA, Hulsen MA, Anderson PD. Numerical simulations of the polydisperse droplet size distribution of disperse blends in complex flow. *Rheologica Acta*. 2021;60(4):187–207. Available from: <https://doi.org/10.1007/s00397-021-01258-4>.
- Han JW, Joo CW, Lee J, Ramadhan ZR, Hong J, Park SB, et al. Enhancement of spectral stability and outcoupling efficiency in organic light-emitting diodes with breath figure patterned microlens array films. *Optical Materials*. 2019;96:109262. Available from: <https://doi.org/10.1016/j.optmat.2019.109262>.
- Kumar V, Dash S. Evaporation-Based Low-Cost Method for the Detection of Adulterant in Milk. *ACS Omega*. 2021;6(41):27200–27207. Available from: <https://doi.org/10.1021/acsomega.1c03887>.
- Carreón YJP, Díaz-Hernández O, Santos GJE, Cipriano-Urbano I, Solorio-Ordaz FJ, González-Gutiérrez J, et al. Texture Analysis of Dried Droplets for the Quality Control of Medicines. *Sensors*. 2021;21(12):1–24. Available from: <https://doi.org/10.3390/s21124048>.
- Bormashenko E, Frenkel M, Vilk A, Legchenkova I, Fedorets AA, Aktaev NE, et al. Characterization of Self-Assembled 2D Patterns with Voronoi Entropy. *Entropy*. 2018;20(12):1–13. Available from: <https://doi.org/10.3390/e20120956>.
- Zhang R, Liao W, Wang Y, Wang Y, Wilson DI, Clarke SM, et al. The growth and shrinkage of water droplets at the oil-solid interface. *Journal of Colloid and Interface Science*. 2021;584:738–748. Available from: <https://doi.org/10.1016/j.jcis.2020.09.102>.
- He C, Zhang P, He Z, Yue L. Analysis of spray characteristics of a jet-film injection element based on Voronoi tessellation. *Acta Astronautica*. 2023;206:100–113. Available from: <https://doi.org/10.1016/j.actaastro.2023.02.006>.

- 16) Honda K, Fujiwara K, Hasegawa K, Kaneko A, Abe Y. Coalescence and mixing dynamics of droplets in acoustic levitation by selective colour imaging and measurement. *Scientific Reports*. 2023;13(1):1–12. Available from: <https://doi.org/10.1038/s41598-023-46008-z>.
- 17) Cheng G, Xuan Z, Tang Z, Tian S, Ding G, Wan X. TiCT MXene modification using silicane or quaternary ammonium salt via covalent bonding or interaction for high-performance composites. *Polymer Composites*. 2023;44(12):8378–8388. Available from: <https://doi.org/10.1002/pc.27704>.
- 18) Schnell G, Polley C, Thomas R, Bartling S, Wagner J, Springer A, et al. How droplets move on laser-structured surfaces: Determination of droplet adhesion forces on nano- and microstructured surfaces. *Journal of Colloid and Interface Science*. 2023;630(Part A):951–964. Available from: <https://doi.org/10.1016/j.jcis.2022.10.091>.
- 19) Bangoura MA, Mimeau D, Balnois E, Réhel K, Azemar F, Linossier I. Impact of Molecular Weight on Anti-Bioadhesion Efficiency of PDMS-Based Coatings. *Coatings*. 2024;14(1):1–15. Available from: <https://doi.org/10.3390/coatings14010149>.
- 20) Liu W, Zhou Z, Liao X, Li C, Tang H, Xie M, et al. Tailoring ordered microporous structure of cellulose-based membranes through molecular hydrophobicity design. *Carbohydrate Polymers*. 2020;229:115425. Available from: <https://doi.org/10.1016/j.carbpol.2019.115425>.
- 21) Gdc P, Marambio OG, Jeria-Orell M, Oyarzún DP, Martín-Trasanco R, Sánchez J. Porous Surface Films with Tunable Morphologies and Hydrophobic Properties Based on Block Copolymer Under the Effects of Thermal Annealing. *Frontiers in Chemistry*. 2019;7:1–9. Available from: <https://doi.org/10.3389/fchem.2019.00181>.
- 22) Huang J, Zhu J, Sun W, Ji J. Versatile and Functional Surface Patterning of in Situ Breath Figure Pore Formation via Solvent Treatment. *ACS Applied Materials & Interfaces*. 2020;12(41):47048–47058. Available from: <https://doi.org/10.1021/acsami.0c14614>.
- 23) Liu W, Li C, Lin X, Xie H, Chen Y, Li Z, et al. Ordered porous films of biomass-based polymers by breath figure: a review. *Cellulose*. 2022;29(12):6463–6491. Available from: <https://doi.org/10.1007/s10570-022-04679-3>.
- 24) Ijaz A, Topcu G, Miko A, Demirel AL. Synergistic control of breath figures on Styrene-Butadiene-Styrene films by poly-2-ethyl-2-oxazoline capped CaCl₂ loaded mesoporous silica particles. *Colloids and Surfaces A: Physicochemical and Engineering Aspects*. 2023;672:131740. Available from: <https://doi.org/10.1016/j.colsurfa.2023.131740>.